

## **Epigenetic upregulation of FKBP5 by aging and stress contributes to NF- $\kappa$ B-driven inflammation and cardiovascular risk**

### **Supplementary Methods**

#### *Human cohorts and clinical measures*

The first main human cohort was derived from the Grady Trauma Project (GTP), a large study conducted in Atlanta, Georgia that investigates how genetic and environmental factors shape stress responses. Participants predominantly come from an African American, urban population of low socioeconomic status (1, 2). This population is characterized by high prevalence and severity of psychosocial stress exposure and is thereby particularly suitable for examining the impact of stress-related phenotypes on genomic regulation. All African American subjects with available *FKBP5* DNA methylation and/or genome-wide gene expression data were included in the analyses. Stress-related phenotypes of interest included depressive symptoms measured with the Beck Depression Inventory (BDI) (3, 4) and childhood trauma with the Childhood Trauma Questionnaire (CTQ) (5). Based on a standard BDI cutoff score (3), subjects were categorized as having higher (total BDI score  $\geq 19$ ) or lower levels (total BDI score  $< 19$ ) of depressive symptoms. Lifetime abuse of substances, including tobacco, alcohol, cannabis, and heroin was assessed with the Kreek-McHugh-Schluger-Kellogg scale (6). Education level in the GTP was defined as highest grade completed, including less than 12<sup>th</sup> grade, high school graduate, GED, some college or technical school, technical school graduate, college graduate, and graduate school. Morning serum cortisol was measured as described previously with a commercial radioimmunoassay kit (Diagnostic Systems Laboratories, Webster, TX, USA) (7). All participants provided written informed consent

and all procedures were approved by the Institutional Review Boards of the Emory University School of Medicine and Grady Memorial Hospital (IRB00002114).

The second main cohort was derived from the Cooperative Health Research in the Region of Augsburg (KORA) F4 community study conducted between 2006 and 2008, a follow-up study of the fourth KORA survey S4 conducted between 1999 and 2001. Individuals of European descent were recruited from the city of Augsburg and two adjacent counties in the south of Germany (8), and DNA methylation was measured in a study subset. Depressive symptoms were assessed with the DEpression and EXhaustion subscale (DEEX scale) of the von Zerrssen symptom checklist (9). Based on a previously defined DEEX cutoff (10), subjects were categorized as having higher (total DEEX score  $\geq 11$ ) or lower levels of depressive symptoms (DEEX score  $< 11$ ). Smoking was defined as current smoker, occasional smoker, former smoker, or never smoker. Education level was documented as the total number of education years. History of diagnosed myocardial infarction (MI) was determined using a self-reported questionnaire. The study has been conducted according to the principles expressed in the Declaration of Helsinki. Written informed consent was given by all participants. All study protocols were reviewed and approved by the local ethics committee (Bayerische Landesärztekammer).

The third main cohort comprised of depressed and control individuals of European descent that were recruited at the Max Planck Institute of Psychiatry (MPIP). Recruitment strategies and characterization of case/control subjects have been previously described (11-13). Briefly, subjects were screened with either the Schedule for Clinical Assessment in Neuropsychiatry or the Composite International Diagnostic Screener, and diagnosis of major depressive disorder was ascertained according to the Diagnostic and Statistical Manual of Mental Disorders (DSM) IV criteria. Education levels documented included no school certificate/graduation, special needs

school, lower secondary school (five years) without certificate, lower secondary school (five years) with certificate, technical secondary school, school certificate after six years of secondary education, or higher school certificate after 8 to 9 years of secondary education. Self-reported history of physician-diagnosed myocardial infarction was documented upon enrollment in the study. Written informed consent was obtained from all subjects, and the study was approved by the ethics committee of the Ludwig-Maximilians-University in Munich.

The impact of severe early life stress on *FKBP5* methylation was examined in a subset of the Helsinki Birth Cohort Study (HBCS) (14). The HBCS has detailed information on the separation of Finnish children from their parents, which occurred during World War II and was documented by the Finnish National Archives registry between 1939 and 1946. The subset with available DNA methylation data includes separated and non-separated (control) males. In the separated subjects' group, the mean age at separation was 4.7 years (SD, 2.4 years) and the mean duration of separation 1.7 years (SD, 1 year). Based on self-report, subjects were categorized as never smokers, former smokers, occasional smokers, and active smokers. The highest level of education was documented, including primary level or less, secondary level, lower tertiary (polytechnic, vocational, or bachelors), and higher tertiary (master's or above). The HBCS was carried out in accordance with the Declaration of Helsinki, and the study protocol was approved by the Institutional Review Board of the National Public Health Institute. Written informed consent was obtained from all participants.

The demographics for all four main participating cohorts and relevant variables are provided in Dataset S1.

*DNA methylation array analyses*

Genomic DNA from the GTP, the MPIP, and the HBCS cohorts was extracted from whole blood using the Genra Puregene Blood Kit (QIAGEN). DNA purity and quantity were assessed by NanoDrop 2000 Spectrophotometer (Thermo Scientific) and Quant-iT Picogreen (Invitrogen). Genomic DNA was bisulfite converted using the Zymo EZ-96 DNA Methylation Kit (Zymo Research) and DNA methylation levels were assessed using the Illumina HumanMethylation450 BeadChip (450K). Hybridization and processing were performed according to the manufacturer's instructions as previously described (15). Quality control of methylation data, including intensity readouts, filtering (detection P value  $> 0.01$  in  $> 50\%$  of the samples), as well as beta and M-value calculation was done using the minfi Bioconductor R package version 1.10.2 (16). Blood cell proportions were calculated using a Minfi-based implementation of the Houseman et al. algorithm (17). We excluded X chromosome, Y chromosome, and non-specific binding probes (18), as well as probes if single nucleotide polymorphisms (SNPs) were documented in the interval for which the Illumina probe is designed to hybridize. Given that the GTP cohort includes individuals from different ethnicities, we also removed probes if they were located close (10bp from query site) to a SNP which had Minor Allele Frequency of  $\geq 0.05$ , as reported in the 1,000 Genomes Project, for any of the populations represented in the samples. All data were normalized with functional normalization (FunNorm) (19), an extension of quantile normalization included in the R package *minfi*. Technical batch effects were identified by inspecting the association of the first principal component of the methylation levels with bisulfite conversion plate, plate position, array, slide, slide row, and slide column, and by further visual inspection of principal component plots using the shinyMethyl Bioconductor R package version 0.99.3 (20). Batch effect removal was then performed with the Combat procedure as implemented in the sva package (21), and the batch-corrected data were used for further analyses.

For the KORA study, genomic DNA (1  $\mu$ g) from 1,814 samples was bisulfite converted using the EZ-96 DNA Methylation Kit (Zymo Research, Orange, CA, USA) according to the manufacturer's protocol, with the incubation conditions recommended for the Illumina Infinium Methylation Assay. Raw methylation data were generated by BeadArray Reader and extracted by GenomeStudio (version 2011.1) with methylation module (version 1.9.0). Data were preprocessed using R version 3.0.1 (<http://www.r-project.org/>) (22). Probes with signals from less than three functional beads and probes with a detection p-value  $> 0.01$  were defined as low-confidence probes. As probe binding might be affected by SNPs in the binding area, CpGs in close proximity (50bp) to SNPs with a minor allele frequency of at least 5% were excluded from the dataset. Color bias adjustment using smooth quantile normalization method as well as background level correction based on negative-control probes present on the Infinium HumanMethylation BeadChip was performed for each chip using the R package lumi (version 2.12.0) (23). Beta values corresponding to low-confidence probes were then set to missing, and samples as well as CpGs were subjected to a 95% detection rate threshold, where samples and CpGs with more than 5% low-confidence probes were removed from the analysis. Finally, beta-mixture quantile normalization (BMIQ) was applied to correct the shift in the distribution of the beta values of the InfI and InfII probes (24). BMIQ was done using the R package wateRmelon (version 1.0.3) (25). Samples were processed on 20 96-well plates in 9 batches; technical batch effects were investigated through principle component and eigen-R2 analysis based on positive control probes (26). Batches were then corrected by including the first principle components as covariates in all regression models.

DNA methylation analyses included 45 CpGs covered by the 450K that are located within or in close proximity (10kb upstream or downstream) to the *FKBP5* locus. All 45 CpGs were

measured in the KORA, whereas one CpG (cg00052684) did not pass quality control in the other cohorts. To rule out unbalanced distribution of the variables of interest that could result in batch effects, we performed chi-squared tests for the distribution of depressive symptom severity, childhood trauma severity, early life separation, and MI across bisulfite conversion plate, slide, slide row, and slide column in all four cohorts; all chi-square p-values were  $> 0.05$ . In all cohorts, we controlled for the potential confounding effect of cell type heterogeneity with a DNA methylation-based approach (17) that employs 450K array data to calculate blood cell proportions and is widely used in most of the large epigenome-wide and other association studies (27, 28) and has been repeatedly validated (29, 30). The calculated blood cell proportions were included as covariates in all DNA methylation analyses. To further rule out the confounding effect of distinctive cell type patterns, we also analyzed DNA methylation data from FACS-sorted CD4 T cells and neutrophils that are publicly available in NCBI GEO (GSE67705) (31). Lastly, we used an additional dataset of male and female subjects ( $n = 213$ ) with both 450K data and differential complete blood counts available at the MPIP. Analytical approaches in this dataset were performed as previously described (32).

#### *Functional annotation of DNA methylation sites*

Annotation of the identified CpGs was performed using the Roadmap Epigenome Browser (<http://epigenomegateway.wustl.edu/browser/roadmap/>) for all available tracks (H3K4me1, H3K4me3, H3K27ac, H3K27me3, H3K9me3, H3K36me3, and methylC-Seq) and for the genetic location surrounding the age/stress-related CpGs (hg19, chr6:35654000-35660000). To assess whether the two sites co-localize with specific chromatin states, we used the 15-state ChromHMM

annotation of the Roadmap Epigenomics project and calculated the position-based overlap of all 15 states among the 127 available epigenomes (33).

### *Gene expression arrays*

Genome-wide gene expression data were measured in 355 African American subjects from the GTP. Whole blood RNA was collected, processed, and hybridized to Illumina HumanHT-12 v3 and v4 Expression BeadChips (Illumina, San Diego, CA, USA) as previously described (15, 34). The raw microarray scan files were exported using the Illumina Beadstudio program 13 and further analyzed in R ([www.R-project.org](http://www.R-project.org)). Microarray data were transformed and normalized via the variance stabilizing normalization with the use of Illumina internal controls (35). Empirical Bayes method was used to control for potential confounding as a result of batch effects (21). Furthermore, to preclude batch effects in analyses involving gene expression data, we tested for possible unbalanced distribution of depressive symptom and childhood trauma severity across amplification and hybridization batches, slide, and sample position using chi-squared tests (all p-values > 0.05). Six pairs of technical replicates were used to confirm data reproducibility (average Pearson correlation 0.996).

### *Population stratification*

The potential confounding by population stratification was controlled using genome-wide SNP data. In the GTP cohort, of the 700K SNPs present on the Omni Quad and Omni express arrays, 645,8315 autosomal SNPs were left after filtering with the following criteria: minor allele frequency of >1 %; Hardy-Weinberg equilibrium of 0.000001; and genotyping rate of >98 %. The

MPIP cohort was genotyped using the Illumina 300k, 610k, and Omni express arrays. For each chip array, quality control was performed separately following the same quality control protocol like in the GTP. After QC, we used the overlap of 168,138 SNPs across all chip types. The samples were clustered to calculate rates of identity by descent (IBD). We then ran multidimensional scaling analysis on the IBD matrix using PLINK2 (<https://www.cog-genomics.org/plink2>) and plotted the first ten axes of variation against each other. No outliers were detected. The first two principal components were used as covariates in regression models to adjust for population stratification.

### *Pathway analyses*

*FKBP5* mRNA levels were correlated with the expression of all genes with at least one array probe detected above background in peripheral blood in the GTP cohort. For genes with more than one probe, gene (mRNA) expression levels were calculated by averaging their levels. Using the set of FDR-corrected genes correlating with *FKBP5* as input and the set of genes expressed above background as reference, we then implemented disease association and transcription factor target analysis using the WEB-based GENE SeT AnaLYsis Toolkit (WebGestalt 2013; [http://www.webgestalt.org/webgestalt\\_2013/](http://www.webgestalt.org/webgestalt_2013/)) (36, 37). Enrichment analysis for disease-associated genes is based on GLAD4U as the source database. Enrichment analysis for the targets of transcription factors is performed using MSigDB as the source database. Both analyses were performed with a hypergeometric test, whereby the minimum number of genes for the enrichment analysis was set at 5. Both analyses were FDR-corrected for multiple testing.

For analysis involving the co-expression network of NF- $\kappa$ B (nuclear factor kappa-light-chain-enhancer of activated B cells), the list of NF- $\kappa$ B-related genes was acquired from the KEGG



Pathway Database ([http://www.genome.jp/dbget-bin/www\\_bget?pathway:hsa04064](http://www.genome.jp/dbget-bin/www_bget?pathway:hsa04064)). Using the gene expression array data in the GTP as described above, the pairwise correlation coefficients between gene pairs encoding molecules that directly interact along the NF- $\kappa$ B pathway were calculated and adjusted for the expression levels of all other pathway partners using the R package GeneNet (38). The adjustment is made by Gaussian Graphical Model (GGM), which measures the degree of association between two genes by controlling for the expression of other genes. For two genes of interest, using the Pearson correlation coefficient will give a misleading result if they are related to another gene(s). A partial correlation coefficient (pcor) measures the degree of association between two random variables after controlling for the effect of a set of random variables. Supposing there are three genes  $x$ ,  $y$ , and  $z$ , the pcor of gene  $x$  and gene  $y$  conditioned on the effect of gene  $z$  is given as:

$$r_{xy;z} = \frac{r_{xy} - r_{xz}r_{yz}}{\sqrt{(1 - r_{xz}^2)(1 - r_{yz}^2)}} ,$$

where  $r_{xy}$ ,  $r_{xz}$ , and  $r_{yz}$  are the standard Pearson product-moment correlation coefficients. Let  $G = \{g_1, \dots, g_m\}$  be the expression matrix of  $m$  genes in a pathway. A pathway-based pcor denotes the pairwise correlation of gene  $x$  and gene  $y$  with the effect of the remaining  $m-2$  genes in the same pathway removed, which is calculated by:

$$r_{xy;m \setminus \{x,y\}} = -\frac{s_{xy}}{\sqrt{s_{xx}s_{yy}}} ,$$

where  $s_{xy}$  is the (x,y) element of the inverse of the correlation matrix. The effect of age, sex, cortisol, and Houseman-calculated blood cell proportions is removed by including the respective variables into G.

These partial pairwise correlations were then compared between subjects with higher and those with lower *FKBP5* expression as defined by a median split of *FKBP5* mRNA levels. To assess the significance of the difference between two correlation coefficients, the coefficients have to be converted to z values using Fisher's z transformation (39). The formula for the transformation is:

$$z(r) = \frac{1}{2} \ln \frac{1-r}{1+r}$$

where ln is the natural logarithm. For sample sizes of  $n_1$  and  $n_2$  find the z of the difference between the z transformed correlations divided by the standard error of the difference of two z scores (<https://CRAN.R-project.org/package=psych> Version = 1.7.8.):

$$z = \frac{z_1 - z_2}{\sqrt{\frac{1}{(n_1 - 3) + (n_2 - 3)}}}$$

Then z is approximately normally distributed with a mean of 0 and a standard deviation of 1. In order to account for multiple testing, we applied FDR correction to obtain a corrected estimate of the significance level. Lastly, to test the robustness of the change in partial correlations between

the two groups, the *FKBP5* high/low group assignments for each pair were permuted 10,000 times across samples.

### *Cell culture*

Cell culture experiments involving immune cells were conducted in peripheral blood mononuclear cells (PBMC), Jurkat (ATCC, TIB-152), or THP-1 (ATCC, TIB-202). For PBMC isolation, the whole blood of healthy volunteers was collected via venipuncture, diluted with PBS, carefully loaded on Biocoll solution (BioChrom, L6113), and centrifuged at 800 g for 20 min without brake. PBMC were enriched by selecting the interphase of the Biocoll gradient and were then washed two times with ice-cold PBS and resuspended in medium. All cells were maintained in RPMI (Gibco) supplemented with 10% FCS and 1% Antibiotic/Antimycotic (Thermo Fisher scientific Inc., Schwerte, Germany). *FKBP5* overexpression in Jurkat cells was performed using a previously described FKBP51-FLAG (40). For all drug treatments of immune cells, cells were left after seeding to rest overnight and were subsequently incubated overnight with vehicle (0.05% DMSO), 25ng/ml Phorbol-12-myristate-13-acetate (Sigma, P1585) and 375ng/ml ionomycin (Sigma, I0634) (PMA/I), 100 nM dexamethasone (DEX; Sigma, D4902), and/or 100 nM SAFit1 as indicated per experiment. Cell transfections with amounts of 2 µg of plasmid DNA were performed using the Amaxa Nucleofector Device and the Cell Line Nucleofector Kit V (Lonza, Basel, Switzerland).

To model replicative senescence *in vitro*, IMR-90 cells (I90-83, Passage 4) were obtained from the Coriell Institute for Medical Research (Camden, New Jersey, USA) and grown in DMEM medium (41966029, Thermo Fisher scientific Inc., Schwerte, Germany) supplemented with

minimum essential medium non-essential amino acids (Thermo Fisher scientific Inc., Schwerte, Germany), 15 % FCS (Thermo Fisher scientific Inc., Schwerte, Germany) and 1 % Antibiotic/Antimycotic in an incubator under 37 °C and 5 % CO<sub>2</sub> conditions. Cells were split at a confluency of 80-90% after a wash step with DPBS (Thermo Fisher scientific Inc., Schwerte, Germany) using Trypsin-EDTA (Thermo Fisher scientific Inc., Schwerte, Germany) incubated for 8-10 min at 37°C. Cells were aged in culture, and replicative age was defined according to the population doubling level (PDL) as either young (PDL = 22) or old (PDL = 42) as previously described (41). To model stress *in vitro*, cells of young and old age (n = 4 replicates each) were split and treated in parallel with either 100nM DEX or vehicle (DMSO) for 7 days. For DNA extraction, cells were pelleted and extracted using the NucleoSpin® Tissue Kit (Macherey-Nagel GmbH & Co.KG, Dueren, GER) following the manufacturer's instructions.

### *Targeted bisulfite sequencing*

To validate the age-related sites using a non-hybridization-based DNA methylation method, we performed targeted bisulfite sequencing using the Illumina MiSeq based on a method we previously described (42). 200 ng to 500 ng of genomic DNA was bisulfite treated using the EZ DNA Methylation Kit (Irvine, California). Target enrichment was achieved by PCR amplification using 20 ng of bisulfite converted DNA, bisulfite specific primer (FKBP5\_TSS\_5.1\_FW:TTTTTGTTTTTTGTGGGGGT; FKBP5\_TSS\_5.1\_RW: AACCTCTTCCTATTTTAATCTC), Takara EpiTaq HS Polymerase (Saint-Germain-en-Laye, France), and the following cycling conditions: 94°C – 3 min, 2x (94°C – 30s, 62.1°C – 30s, 72°C – 30s), 5x (94°C – 30s, 60.1°C – 30s, 72°C – 30s), 8x (94°C – 30s, 58.1°C – 30s, 72°C – 30s), 34x (94°C – 30s, 56.1°C – 30s, 72°C – 30s), 72°C – 5 min, 4°C – ∞. Equimolar pooled amplicons of

each sample were cleaned up by a double size selection (200-500 bp) using Ampure XP beads (Krefeld, Germany). The Illumina TruSeq DNA PCR-Free HT Library Prep Kit (San Diego, California) was used for library generation according to the manufacturer's instructions. Paired-end sequencing was performed on an Illumina MiSeq Instrument (San Diego, California) with the MiSeq Reagent Kit v3 (2 x 300-cycles) with the addition of 30% of PhiX Library. The quality of sequencing reads was performed with FastQC (<http://www.bioinformatics.babraham.ac.uk/projects/fastqc>). After trimming Illumina adapter sequences with Cutadapt v1.9.1, Bismark v.0.15.0 was used for the alignment to a restricted reference that was based on the PCR targets. An in-house Perl script was used to stitch paired-end reads and remove low quality ends of paired-end reads if they overlapped. The methylation levels for all CpGs, CHGs, and CHHs were quantified using the R package methylKit. Subsequently, a three-step quality control was utilized to validate the methylation calls. First, PCR artifacts introducing CpGs at 0 or 100% methylation level were removed. Second, CHH methylation levels were analyzed, and samples with insufficient bisulfite conversion rate (< 95%) were removed. Finally, CpG sites with coverage lower than 1000 reads were excluded.

For DNA methylation measurements in IMR-90 cells, *FKBP5* methylation of CpG sites corresponding to 450K cg20813384 and cg00130530 (Chr6: 35657180 & Chr6:35657202, respectively; Assembly: hg19) was assessed by targeted bisulfite pyrosequencing in four biological replicates. For each replicate, 500 ng genomic DNA was bisulfite converted using the EZ DNA Methylation Kit (Zymo Research Corporation, CA, USA). Bisulfite converted DNA was amplified in a 50 µl reaction mix (1 µl DNA; each bisulfite specific Primer with a final concentration of 0.2 µM, *FKBP5\_TSS\_5\_F*: TTTTGT TTTTGTGGGGT & *FKBP5\_TSS5\_R\_biot*: biotin-AACCTCTTCCTATTTAATCTC) using the Takara EpiTaq HS Polymerase (Clontech, Saint-

Germain-en-Laye, France). Cycling conditions of the touchdown PCR were 94°C for 3 min, 2x (94°C - 30s, 62.1 °C - 30s, 72°C - 30s), 5x (94°C - 30s, 60.1 °C - 30s, 72°C - 30s), 8x (94°C - 30s, 58.1 °C - 30s, 72°C - 30s), 34x (94°C - 30s, 56.1 °C - 30s, 72°C - 30s), 72°C for 5 min, and cooling to 4°C. Pretreatment of PCR amplicons was facilitated with the PyroMark Q96 Vacuum Workstation (QIAGEN GmbH, Hilden). Sequencing of FKBP5 CpGs was performed on a PyroMark Q96 ID system (QIAGEN GmbH, Hilden) using PyroMark Gold Q96 reagents and the following sequencing Primer: FKBP5\_TSS\_5\_Seq1 (CpG 35657180, 35657202 / hg19): AATTTTATTAAGTTTAAGATGTTTA. The PyroMark Q96 ID Software 2.5 (QIAGEN GmbH, Hilden) was used for data analysis.

#### *Generation of FKBP5 knockout Jurkat cells*

Jurkat cells were transfected with a pool of three clustered regularly interspaced short palindromic repeats-associated Cas 9 (CRISPR/Cas9) plasmids containing gRNA that targets human *FKBP5* and a GFP reporter (Santa Cruz, sc-401560). 36 hours post transfection, cells were FACS-sorted for GFP as single cells into a 96-well plate using BD FACSAria III. Single clones were expanded and Western blotting was used to confirm the successful knockout of *FKBP5*.

#### *Co-immunoprecipitation experiments (CoIPs)*

CoIPs of endogenous or FLAG-tagged FKBP5 with endogenous IKK $\alpha$  and NIK were performed in Jurkat cells and PBMC using previously described methods (43).  $5 \times 10^6$  cells were transfected with 2  $\mu$ g of the respective expression plasmids. After 3 days of cultivation in medium, cells were lysed in CoIP buffer containing 20 mM Tris-HCl (pH 8.0), 100 mM NaCl, 1 mM EDTA, and 0.5%

Igepal, complemented with protease inhibitor cocktail (Roche). This was followed by incubation on an overhead shaker for 20 min at 4°C. The lysate was cleared by centrifugation, the protein concentration was determined by performing a BCA assay, and 1.2 mg of lysate was incubated with 2.5 µg of FLAG antibody overnight at 4°C. 20 µl of BSA-blocked Protein G Dynabeads (Invitrogen, 100-03D) were added to the lysate-antibody mix, followed by 3 h of incubation at 4°C. The beads were washed three times with PBS, and protein-antibody complexes were eluted with 100 µl of 1 x FLAG-peptide solution (Sigma, 100–200 µg/ml, F3290) in CoIP buffer for 30 min at 4°C. 5–15 µg of the cell lysates or 2.5 µl of the immunoprecipitates was separated by SDS-PAGE and electrotransferred onto nitrocellulose membranes (Western blotting). Opto-densimetric determination of immunodetected bands was carried out on ChemiDoc MP (BioRad). Signals of co-immunoprecipitated proteins were normalized to signals of input-corrected immunoprecipitated proteins.

#### *In vitro DNA methylation*

*In vitro* DNA methylation of biotinylated probes and reporter constructs (detailed sequences in Fig. S9) was carried out by *SssI* CpG Methyltransferase (New England Biolabs, M0226S) according to the manufacturer's instructions. Successful methylation at cg00130530 was confirmed by restriction digest with *XhoI* (recognition sequence: CTCGAG), whereby plasmid digestion is blocked by CpG methylation. Restriction digests were controlled by agarose gel electrophoresis. Furthermore, methylation at cg20813374 was confirmed and quantified using targeted bisulfite pyrosequencing, whereby our *in vitro* protocol induced 91% DNA methylation. Methylated and unmethylated constructs were subsequently transfected into THP-1 cells as

described below. Controls underwent the same procedure except that enzyme and SAM was not added to the reaction.

#### *Biotinylated oligonucleotide-mediated chromatin immunoprecipitation (ChIP)*

Biotinylated oligonucleotide-mediated ChIP was performed in THP-1 cells using a previously established method (44) (schematically outlined in Fig. 5B). Briefly, single-stranded complementary biotinylated oligonucleotide probes (length 70 bp) including the DNA methylation sites and response element of interest (Fig. S9) were synthesized (Eurofins Genomics, Ebersberg, Germany), and after annealing underwent *in vitro* DNA methylation as described above. Subsequently, 0.5 pmol/10<sup>6</sup> cells of either the methylated or unmethylated probes were transfected into THP-1 cells (1.5-2 x 10<sup>6</sup> cells per replicate). After an overnight rest, the cells were incubated for 24 hours at 37°C with either vehicle (DMSO) or PMA/I (concentrations as above), a stimulus that robustly induces NF-κB signaling. Cells subsequently underwent cross-linking with 1% formaldehyde at room temperature for 15% and were then lysed in RIPA buffer (Merck, 20-188, completed with protease inhibitor cocktail). Lysates were immunoprecipitated using streptavidin-coupled magnetic beads (Dynabeads M-280, Thermo Scientific, 11205D) or control beads (Protein G Dynabeads, Thermo Scientific, 10007D), and both input and eluates were quantified for NF-κB/p65 binding by Western blotting.

#### *Western Blot Analysis*

Unless otherwise indicated, protein extracts were obtained by lysing cells in 62.5 mM Tris, 2% SDS, and 10% sucrose, supplemented with protease inhibitors (Sigma, P2714) and phosphatase



inhibitors (Roche, 04906837001). Samples were sonicated and heated at 95°C for 5 min. Proteins were separated by SDS-PAGE and electro-transferred onto nitrocellulose membranes. Blots were placed in Tris-buffered saline (TBS; 50 mM Tris-Cl, pH 7.6; 150 mM NaCl), supplemented with 0.05% Tween (Sigma, P2287) and 5% non-fat milk for 1 h at room temperature and then incubated with primary antibody (diluted in TBS/0.05% Tween) overnight at 4°C. The following primary antibodies were used: FLAG (1:7,000, Rockland, 600-401-383), FKBP5/FKBP51 (1:1,000, Bethyl, A301-430A; 1:1000, Cell Signaling, #8245), NF- $\kappa$ B/p65 (1:1000, Cell Signaling, #8242), IKK $\alpha$  (1:1000, Cell Signaling, #2682), pIKK $\alpha$ <sup>S176</sup> (1:1000, Cell Signaling, #2078), NIK (1:1000, Cell Signaling, #4994), and Actin (1:5,000, Santa Cruz, sc-1616). Subsequently, the blots were washed and probed with the respective horseradish-peroxidase or fluorophore-conjugated secondary antibody for 2 h at room temperature. The immuno-reactive bands were visualized either by using ECL detection reagent (Millipore, WBKL0500) or directly by excitation of the respective fluorophore. Recording of the band intensities was performed with the ChemiDoc MP system from Bio-Rad. All protein data were normalized to Actin, which was detected on the same blot in the same lane (multiplexing). In the case of IKK $\alpha$  phosphorylation and to rule out confounding by changes in total IKK $\alpha$  levels, we normalized pIKK $\alpha$  by calculating its ratio to total IKK $\alpha$ . Results were indistinguishable when pIKK $\alpha$  was normalized to Actin.

#### *Dual-luciferase reporter gene assays*

The functional effect of differential methylation in the age/stress-related *FKBP5* site was analyzed using a CpG-free luciferase reporter vector (45) that was kindly provided by Prof. Michael Rehli, University of Regensburg, Germany. The genomic region of interest (length 224 bp; Fig. S9) was

synthesized and inserted into the *SpeI* and *PstI* sites of the CpG-free vector plasmid, and all constructs were verified by sequencing (Eurofins Genomics, Ebersberg, Germany). THP-1 cells were transfected with either methylated or unmethylated reporter plasmid (800 ng/10<sup>6</sup> cells) and with the previously described *Gaussia*-KDEL control plasmid (100 ng/10<sup>6</sup> cells) (46). To control for differences in transfection efficiency, the NF- $\kappa$ B-driven reporter gene activity was calculated as the ratio of firefly (*Photinus Pyralis*) to *Gaussia* luciferase signals.

To assess the impact of *FKBP5* overexpression on NF- $\kappa$ B activity, 1 x 10<sup>6</sup> Jurkat cells were transfected with NF- $\kappa$ B luciferase reporter (1  $\mu$ g, Promega, E8491) and Renilla (300 ng, Promega, E6921) control plasmids, as well as with either FKBP5-FLAG (1  $\mu$ g) or control vector (pRK5; 1  $\mu$ g). Immediately after transfection, cells were seeded on 96-well plates at a density of 20,000 cells/well and were left to rest overnight. On the next day, cells were incubated for 2 hours with DMSO vehicle or 100nM SAFit1 and were then stimulated overnight with PMA/I (concentration as above). Cells were then lysed in lysis buffer (Promega, E1941) and Firefly and Renilla luciferase activities were recorded with the TriStar<sup>2</sup> S LB 942 microplate reader (Berthold, Bad Wildbad, Germany) following a previously described protocol (47). To control for differences in transfection efficiency, the NF- $\kappa$ B-driven reporter gene activity was calculated as the ratio of firefly to *Renilla* luciferase signals. For each experiment, fold ratios of NF- $\kappa$ B activity were calculated by comparison to cells expressing the control vector.

#### *Enzyme-linked immunosorbent assay (ELISA) for human interleukin-8 (IL-8)*

1 x 10<sup>6</sup> Jurkat cells were transfected with either FKBP5-FLAG (1  $\mu$ g) or control vector (1  $\mu$ g), were seeded in 24-well plates at a density of 500,000 cells/well and, after overnight rest, were stimulated with PMA/I (concentration as above). Supernatants were collected the next day, cleared

by centrifugation at 125g, and stored at -80°C until IL-8 measurement with ELISA, which was performed with a commercially available kit (Merck Millipore, EZHIL8) according to the manufacturer's instructions.

### *Statistics*

All statistical analyses involving DNA methylation used M-values that are thought to be statistically superior to Beta-values (48). To average the methylation levels of the two age-related *FKBP5* CpGs, we calculated the mean of the respective Beta-values and then transformed Beta-value means to the corresponding M-values as previously suggested (48). All p values reporting the statistical significance of DNA methylation analyses originate from tests using M-values, and the residuals from the respective regression models are shown on the main figures; however, to more intuitively depict methylation results, supplementary figures also show the DNA methylation Beta-values for selected panels.

Linear regression models examined the effect of age and stress-related phenotypes on DNA methylation, while including as covariates all the potential confounders that were available in the respective cohorts. Covariates used in each cohort were as follows: age, sex, blood cell proportions, the first two genome-wide SNP-based principal components, and smoking and other substance use in the GTP cohort; age, sex, blood cell proportions, smoking status, and the first two Eigen-R2-derived principal components in the KORA cohort; age, sex, case/control status, blood cell proportions, and the first two genome-wide SNP-based principal components in the MPIP cohort; and age, smoking status, and blood cell proportions in the HBCS cohort. The model validating the association of age with the age-related CpGs using targeted bisulfite sequencing in a small sample of female subjects was adjusted for smoking and blood cell proportions. Linear

regression models examining effects on *FKBP5* expression in the GTP cohort included as covariates age, sex, the first two SNP-based principal components, and blood cell proportions; these models tested methylation of the age/stress-related *FKBP5* CpGs, age, stress-related phenotypes, and cortisol as the independent variables of interest. All stratified analyses in the GTP cohort were performed using median splits in order to maximize statistical power and balance between comparison groups and given that, to the best of our knowledge, there is no scientific justification for otherwise dividing the data. More specifically, median splits were performed for methylation levels of the age/stress-related *FKBP5* CpGs to distinguish subjects with higher vs. lower methylation, for CTQ scores to stratify for childhood trauma severity, for chronological age, and for *FKBP5* mRNA levels. Lastly, we examined the association of history for MI with methylation of the age/stress-related CpGs in the KORA and MPIP cohorts. To account for the case/control imbalance in our MI data, we calculated and controlled for propensity scores for MI assignment using the *twang* package in R with the number of iterations set to 10,000 (<https://cran.r-project.org/web/packages/twang/vignettes/twang.pdf>) (49). Propensity scores were adjusted for age, sex, blood cell proportions, depression status, and the first two principle components in both cohorts, as well as smoking in the KORA. Analyses examining effects on *FKBP5* methylation were further adjusted for education, a measure of socioeconomic status shown to influence DNA methylation (50-53); this additional adjustment did not change any of the results. All p-values reporting the statistical significance of regression models in the main text are after correction for relevant covariates as described above.

Experimental data were normally distributed and were tested using student's t-test when comparing two groups and with two-way analysis of variance (ANOVA) when examining two

factors of interest. Significant effects in the two-way ANOVA were followed with Bonferroni-corrected pairwise comparisons.

Experimental data were analyzed in Sigma Plot version 13.0 (Systat Software Inc.). All other statistical tests were performed in R version 3.1.0 (<http://www.r-project.org/>) (22). Meta-analysis was performed using the package *rmeta* in R, which combines the regression coefficients and standard errors from individual cohorts. The level of statistical significance was set a priori at 0.05 ( $5 \times 10^{-2}$ ). All reported p values are two-tailed and nominal, unless corrected for multiple testing or permutation-based as indicated and reported in the manuscript.

#### *Data sharing and public access*

For the GTP study, we have previously deposited to NCBI GEO both the raw DNA methylation array data (GSE72680) and raw gene expression array data (GSE58137). For the KORA cohort, the informed consents given by study participants do not cover data posting in public databases, but data are available upon request from KORA-gen (<https://epi.helmholtz-muenchen.de/>). Data requests can be submitted online and are subject to approval by the KORA Board. For the MPIP cohort, the raw DNA methylation data and associated phenotypes have been deposited to NCBI GEO (GSE128235). For the HBCS cohort, online data deposition is not compatible with the policies of the University of Helsinki, which complies with the European Union's General Data Protection Regulation and considers any coded data pseudonymized but not anonymized. Interested researchers can obtain a de-identified dataset after obtaining approval from the study board, and data requests may be subject to further review by the national register authority and by the ethics committees.

## References

1. Binder EB, *et al.* (2008) Association of FKBP5 polymorphisms and childhood abuse with risk of posttraumatic stress disorder symptoms in adults. *JAMA : the journal of the American Medical Association* 299(11):1291-1305.
2. Gillespie CF, *et al.* (2009) Trauma exposure and stress-related disorders in inner city primary care patients. *General hospital psychiatry* 31(6):505-514.
3. Beck AT, Steer RA, & Garbin MG (1988) Psychometric Properties of the Beck Depression Inventory - 25 Years of Evaluation. *Clin Psychol Rev* 8(1):77-100.
4. Beck AT, Ward CH, Mendelson M, Mock J, & Erbaugh J (1961) An inventory for measuring depression. *Archives of general psychiatry* 4:561-571.
5. Bernstein DP, *et al.* (2003) Development and validation of a brief screening version of the Childhood Trauma Questionnaire. *Child abuse & neglect* 27(2):169-190.
6. Kellogg SH, *et al.* (2003) The Kreek-McHugh-Schluger-Kellogg scale: a new, rapid method for quantifying substance abuse and its possible applications. *Drug and alcohol dependence* 69(2):137-150.
7. Kaminsky Z, *et al.* (2015) Epigenetic and genetic variation at SKA2 predict suicidal behavior and post-traumatic stress disorder. *Translational psychiatry* 5:e627.
8. Holle R, Happich M, Lowel H, & Wichmann HE (2005) KORA--a research platform for population based health research. *Gesundheitswesen (Bundesverband der Arzte des Offentlichen Gesundheitsdienstes (Germany))* 67 Suppl 1:S19-25.
9. Ladwig KH, Marten-Mittag B, Baumert J, Lowel H, & Doring A (2004) Case-finding for depressive and exhausted mood in the general population: reliability and validity of a symptom-driven diagnostic scale. Results from the prospective MONICA/KORA Augsburg Study. *Annals of epidemiology* 14(5):332-338.
10. Hafner S, *et al.* (2011) Association between social isolation and inflammatory markers in depressed and non-depressed individuals: results from the MONICA/KORA study. *Brain, behavior, and immunity* 25(8):1701-1707.
11. Heck A, *et al.* (2009) Investigation of 17 candidate genes for personality traits confirms effects of the HTR2A gene on novelty seeking. *Genes, brain, and behavior* 8(4):464-472.
12. Kohli MA, *et al.* (2011) The neuronal transporter gene SLC6A15 confers risk to major depression. *Neuron* 70(2):252-265.
13. Lucae S, *et al.* (2006) P2RX7, a gene coding for a purinergic ligand-gated ion channel, is associated with major depressive disorder. *Human molecular genetics* 15(16):2438-2445.
14. Barker DJ, Osmond C, Forsen TJ, Kajantie E, & Eriksson JG (2005) Trajectories of growth among children who have coronary events as adults. *The New England journal of medicine* 353(17):1802-1809.
15. Mehta D, *et al.* (2013) Childhood maltreatment is associated with distinct genomic and epigenetic profiles in posttraumatic stress disorder. *Proceedings of the National Academy of Sciences of the United States of America* 110(20):8302-8307.
16. Aryee MJ, *et al.* (2014) Minfi: a flexible and comprehensive Bioconductor package for the analysis of Infinium DNA methylation microarrays. *Bioinformatics (Oxford, England)* 30(10):1363-1369.
17. Houseman EA, *et al.* (2012) DNA methylation arrays as surrogate measures of cell mixture distribution. *BMC bioinformatics* 13:86.

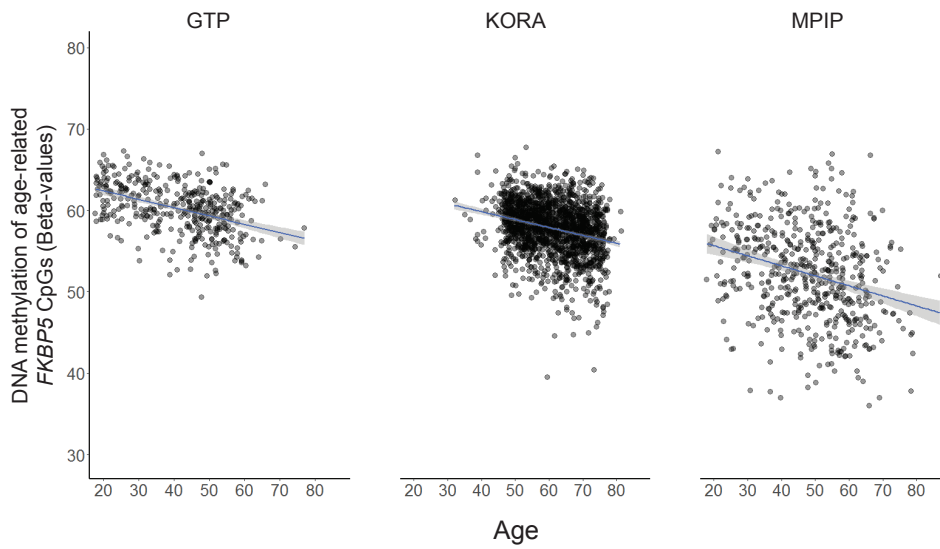
18. Chen YA, *et al.* (2013) Discovery of cross-reactive probes and polymorphic CpGs in the Illumina Infinium HumanMethylation450 microarray. *Epigenetics : official journal of the DNA Methylation Society* 8(2):203-209.
19. Fortin JP, *et al.* (2014) Functional normalization of 450k methylation array data improves replication in large cancer studies. *Genome biology* 15(12):503.
20. Fortin JP, Fertig E, & Hansen K (2014) shinyMethyl: interactive quality control of Illumina 450k DNA methylation arrays in R. *F1000Research* 3:175.
21. Johnson WE, Li C, & Rabinovic A (2007) Adjusting batch effects in microarray expression data using empirical Bayes methods. *Biostatistics* 8(1):118-127.
22. Team RC (2014) A Language and Environment for Statistical Computing. *R Foundation for Statistical Computing, Vienna, Austria.*
23. Du P, Kibbe WA, & Lin SM (2008) lumi: a pipeline for processing Illumina microarray. *Bioinformatics (Oxford, England)* 24(13):1547-1548.
24. Teschendorff AE, *et al.* (2013) A beta-mixture quantile normalization method for correcting probe design bias in Illumina Infinium 450 k DNA methylation data. *Bioinformatics (Oxford, England)* 29(2):189-196.
25. Pidsley R, *et al.* (2013) A data-driven approach to preprocessing Illumina 450K methylation array data. *BMC genomics* 14:293.
26. Chen LS & Storey JD (2008) Eigen-R2 for dissecting variation in high-dimensional studies. *Bioinformatics* 24(19):2260-2262.
27. Wahl S, *et al.* (2017) Epigenome-wide association study of body mass index, and the adverse outcomes of adiposity. *Nature* 541(7635):81-86.
28. Liang L, *et al.* (2015) An epigenome-wide association study of total serum immunoglobulin E concentration. *Nature* 520(7549):670-674.
29. Koestler DC, *et al.* (2013) Blood-based profiles of DNA methylation predict the underlying distribution of cell types: a validation analysis. *Epigenetics : official journal of the DNA Methylation Society* 8(8):816-826.
30. Accomando WP, Wiencke JK, Houseman EA, Nelson HH, & Kelsey KT (2014) Quantitative reconstruction of leukocyte subsets using DNA methylation. *Genome biology* 15(3):R50.
31. Gross AM, *et al.* (2016) Methylome-wide Analysis of Chronic HIV Infection Reveals Five-Year Increase in Biological Age and Epigenetic Targeting of HLA. *Molecular cell* 62(2):157-168.
32. Zannas AS, *et al.* (2015) Lifetime stress accelerates epigenetic aging in an urban, African American cohort: relevance of glucocorticoid signaling. *Genome biology* 16(1):266.
33. Ernst J & Kellis M (2012) ChromHMM: automating chromatin-state discovery and characterization. *Nature methods* 9(3):215-216.
34. Menke A, *et al.* (2012) Dexamethasone stimulated gene expression in peripheral blood is a sensitive marker for glucocorticoid receptor resistance in depressed patients. *Neuropsychopharmacology : official publication of the American College of Neuropsychopharmacology* 37(6):1455-1464.
35. Huber W, von Heydebreck A, Sultmann H, Poustka A, & Vingron M (2002) Variance stabilization applied to microarray data calibration and to the quantification of differential expression. *Bioinformatics (Oxford, England)* 18 Suppl 1:S96-104.
36. Wang J, Duncan D, Shi Z, & Zhang B (2013) WEB-based GENE SeT AnaLysis Toolkit (WebGestalt): update 2013. *Nucleic acids research* 41(Web Server issue):W77-83.
37. Zhang B, Kirov S, & Snoddy J (2005) WebGestalt: an integrated system for exploring gene sets in various biological contexts. *Nucleic acids research* 33(Web Server issue):W741-748.
38. Schafer J & Strimmer K (2005) An empirical Bayes approach to inferring large-scale gene association networks. *Bioinformatics (Oxford, England)* 21(6):754-764.

39. Krumsiek J, Suhre K, Illig T, Adamski J, & Theis FJ (2011) Gaussian graphical modeling reconstructs pathway reactions from high-throughput metabolomics data. *BMC Syst Biol* 5:21.
40. Wochnik GM, *et al.* (2005) FK506-binding proteins 51 and 52 differentially regulate dynein interaction and nuclear translocation of the glucocorticoid receptor in mammalian cells. *The Journal of biological chemistry* 280(6):4609-4616.
41. Kern A, Roempp B, Prager K, Walter J, & Behl C (2006) Down-regulation of endogenous amyloid precursor protein processing due to cellular aging. *The Journal of biological chemistry* 281(5):2405-2413.
42. Roeh S, *et al.* (2018) HAM-TBS: high-accuracy methylation measurements via targeted bisulfite sequencing. *Epigenetics & chromatin* 11(1):39.
43. Gassen NC, *et al.* (2014) Association of FKBP51 with priming of autophagy pathways and mediation of antidepressant treatment response: evidence in cells, mice, and humans. *PLoS medicine* 11(11):e1001755.
44. Ibrahim EE, Babaei-Jadidi R, & Nateri AS (2013) The streptavidin/biotinylated DNA/protein bound complex protocol for determining the association of c-JUN protein with NANOG promoter. *Current protocols in stem cell biology* Chapter 1:Unit 1B.10.
45. Klug M & Rehli M (2006) Functional analysis of promoter CpG methylation using a CpG-free luciferase reporter vector. *Epigenetics : official journal of the DNA Methylation Society* 1(3):127-130.
46. Schulke JP, *et al.* (2010) Differential impact of tetratricopeptide repeat proteins on the steroid hormone receptors. *PloS one* 5(7):e11717.
47. Hampf M & Gossen M (2006) A protocol for combined Photinus and Renilla luciferase quantification compatible with protein assays. *Analytical biochemistry* 356(1):94-99.
48. Du P, *et al.* (2010) Comparison of Beta-value and M-value methods for quantifying methylation levels by microarray analysis. *BMC bioinformatics* 11:587.
49. Rosenbaum P & Rubin D (1983) The Central Role of the Propensity Score in Observational Studies for Causal Effects. *Biometrika* 70(1):41-55.
50. Appleton AA, *et al.* (2013) Patterning in placental 11-B hydroxysteroid dehydrogenase methylation according to prenatal socioeconomic adversity. *PloS one* 8(9):e74691.
51. Borghol N, *et al.* (2012) Associations with early-life socio-economic position in adult DNA methylation. *International journal of epidemiology* 41(1):62-74.
52. Lam LL, *et al.* (2012) Factors underlying variable DNA methylation in a human community cohort. *Proceedings of the National Academy of Sciences of the United States of America* 109 Suppl 2:17253-17260.
53. Needham BL, *et al.* (2015) Life course socioeconomic status and DNA methylation in genes related to stress reactivity and inflammation: The multi-ethnic study of atherosclerosis. *Epigenetics : official journal of the DNA Methylation Society* 10(10):958-969.

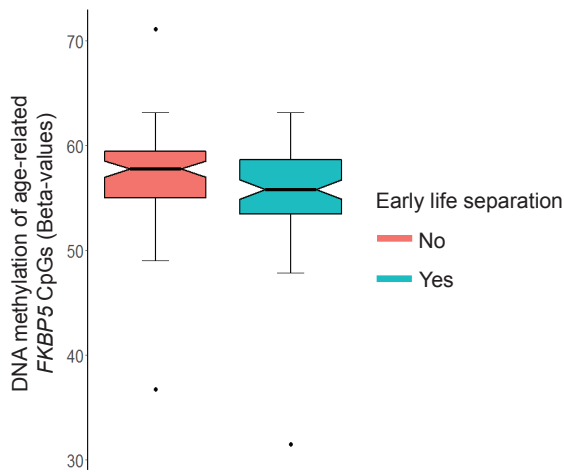


**Figure S1**

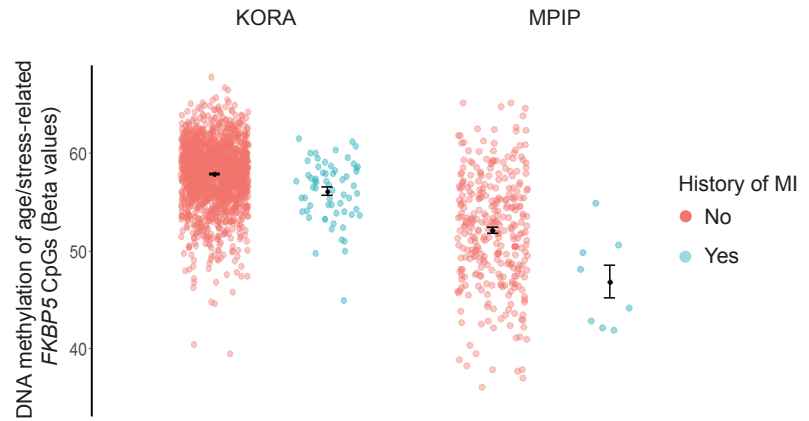
**A**



**B**

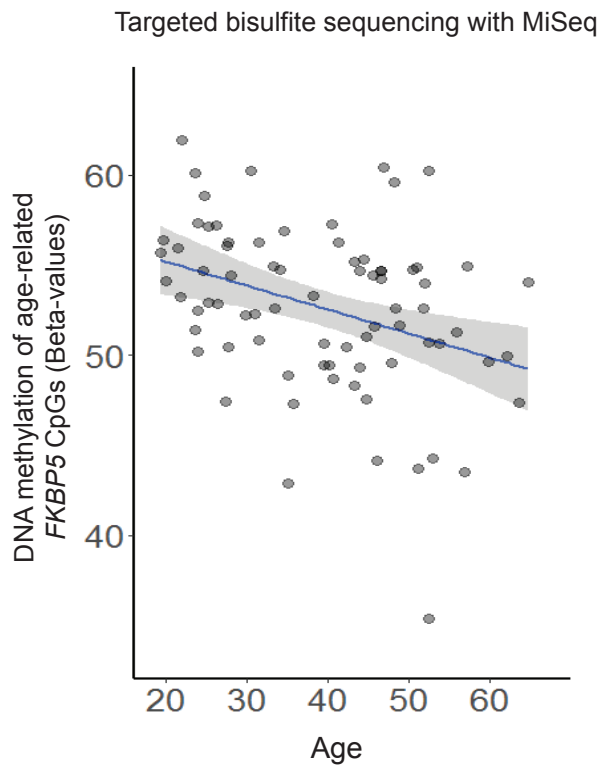


**C**



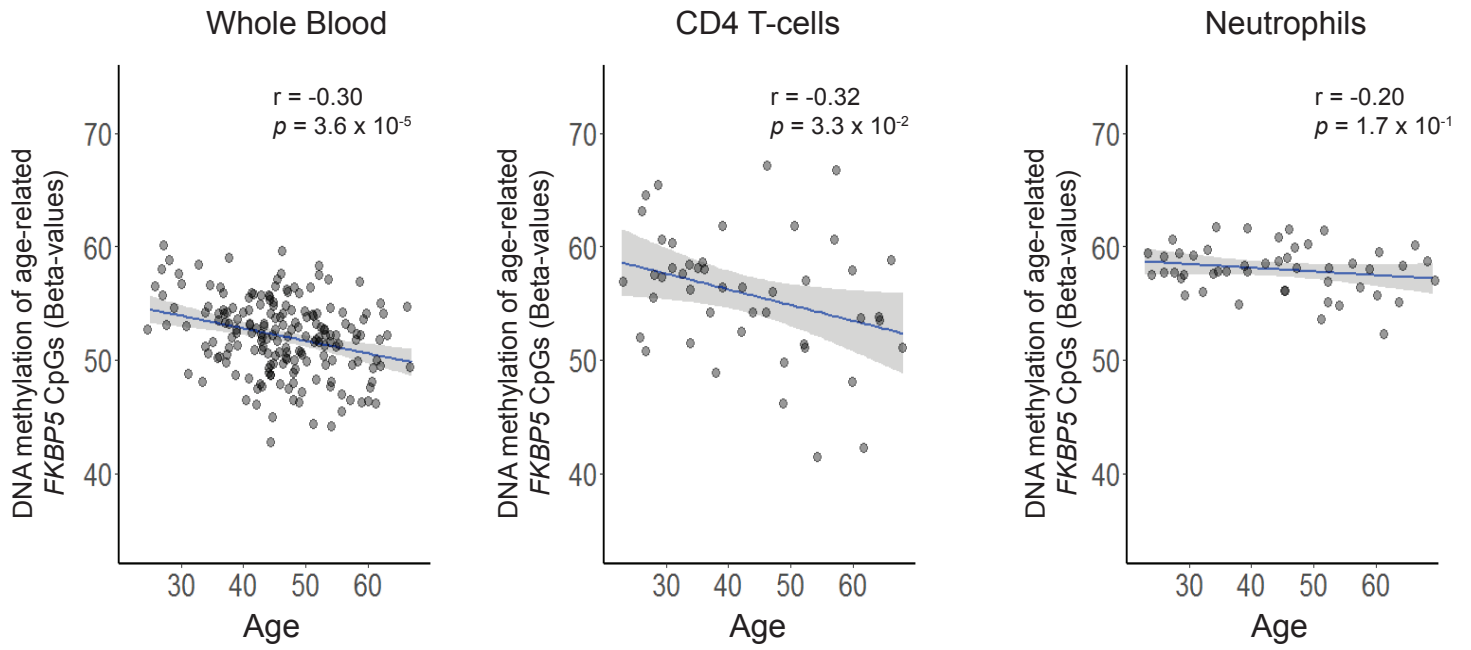
Complementary figure demonstrating how % *FKBP5* DNA methylation levels are associated with aging, early life separation, and history of myocardial infarction. The y axis in all panels depicts the average % DNA methylation (Beta-values) of the two age/stress-related *FKBP5* CpGs (cg20813374 and cg00130530). Further details and statistics are provided in Figures 1 and 6. GTP, Grady Trauma Project; HBCS, Helsinki Birth Cohort Study; KORA, Cooperative Health Research in the Region of Augsburg F4 community study; MI, myocardial infarction; MPIP, Max Planck Institute of Psychiatry depression case/control study.

**Figure S2**



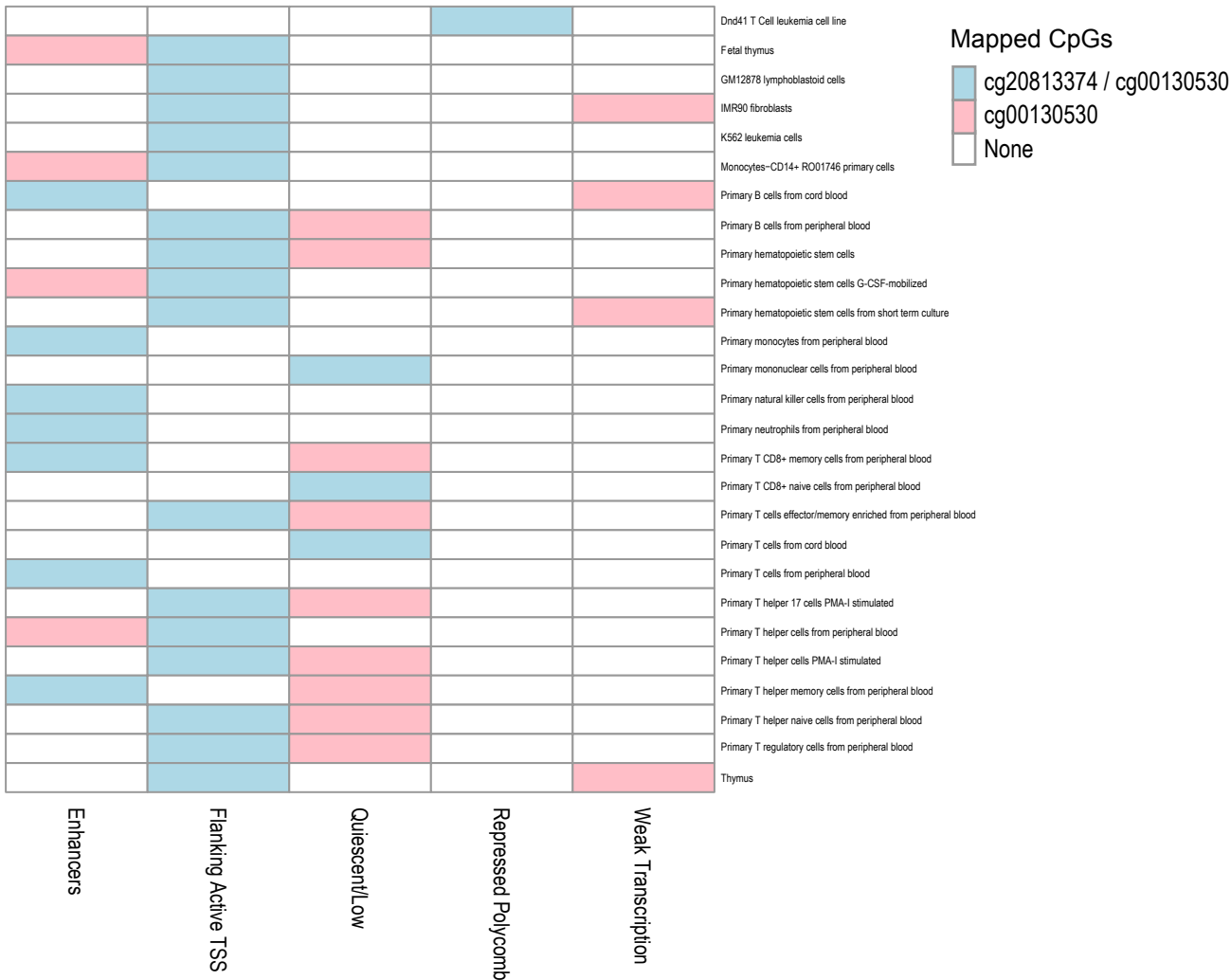
Validation of the 450K-identified age-related *FKBP5* CpGs (cg20813374 and cg00130530) using targeted bisulfite sequencing with the Illumina MiSeq in a sample of female subjects ( $n = 77$ ,  $\beta_{\text{age}} = -0.0074$ ,  $\text{SE} = 0.0031$ ,  $p = 1.9 \times 10^{-2}$ ). The y axis depicts the average % DNA methylation (Beta-values) of the two *FKBP5* CpGs. Reported statistics are after correcting for potential confounders (see Supplementary Methods).

**Figure S3**



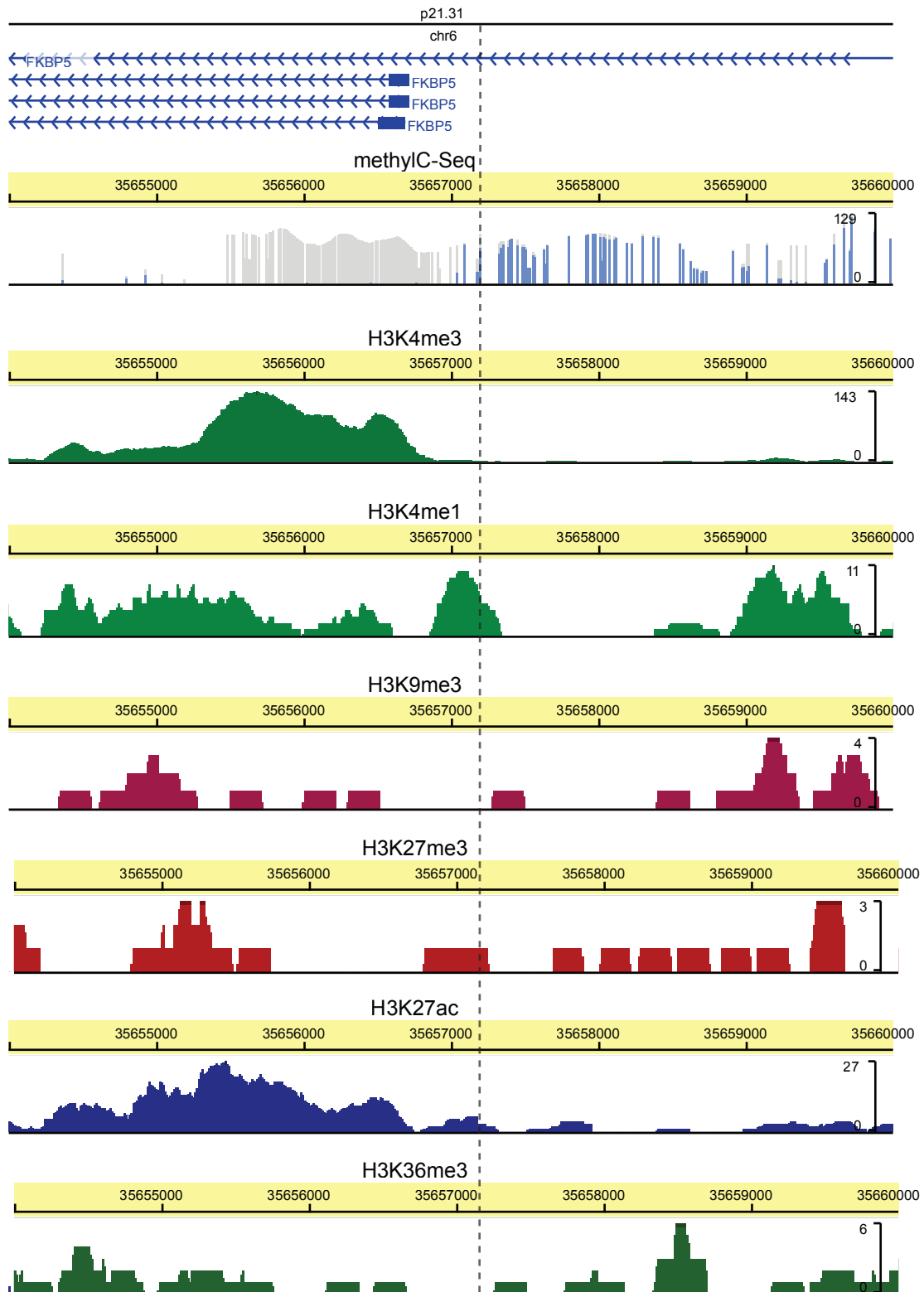
Pearson correlations between age and average methylation of the two age-related CpGs (cg20813374 and cg00130530) using publicly available DNA methylation data in whole blood ( $n = 184$ ), as well as FACS-sorted CD4 T-cells ( $n = 46$ ) and neutrophils ( $n = 48$ ), from male subjects with a broad age range (source: GEO accession number GSE67705).

# Figure S4



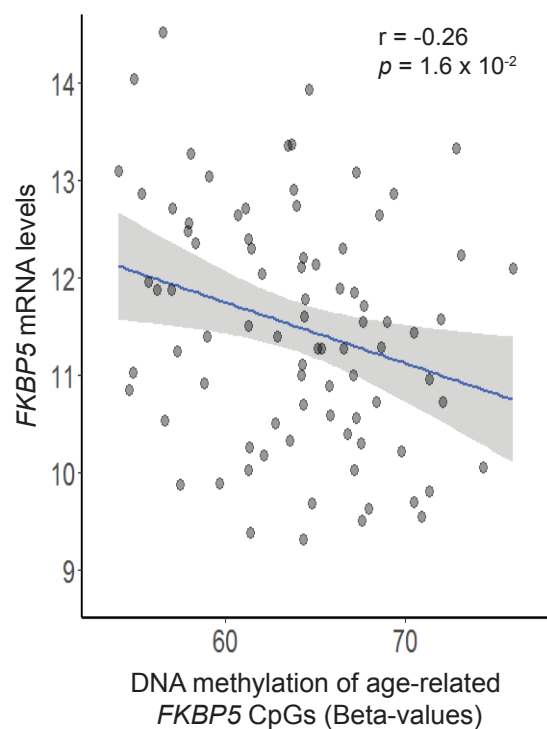
Visual depiction of integrative analysis of chromatin states using ChromHMM within immune cell types, as well as in the IMR-90 fibroblasts that were used as a model of human replicative senescence. Across these cell types, the age/stress-related *FKBP5* CpGs are commonly mapped to an enhancer or flanking active TSS.

Figure S5



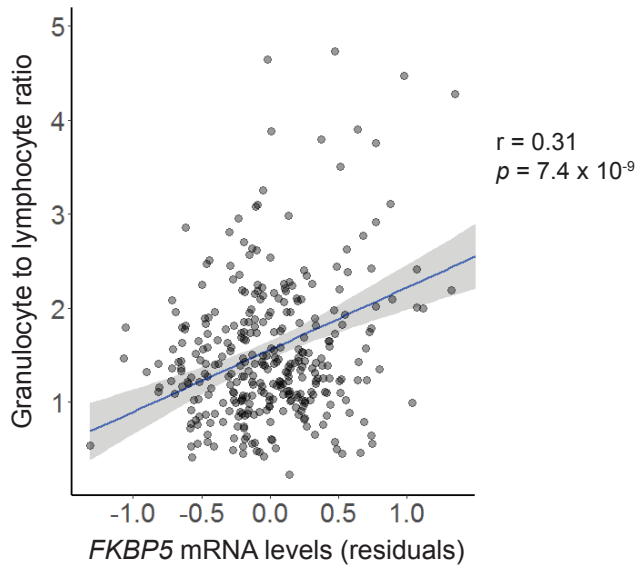
Functional annotation of the *FKBP5* locus at and around the age/stress-related *FKBP5* CpGs, using the Roadmap Epigenome Browser and the “Mobilized CD34 Primary cells” track as a proxy for peripheral immune cells. The two CpGs (cg20813374 and cg00130530) are respectively located at positions 35657180 and 35657202 of chromosome 6 (exact location indicated by dotted line) and, as shown, exhibit intermediate methylation levels and colocalize with H3K4me1 and H3K27me3 signatures. This landscape is most consistent with a poised enhancer.

**Figure S6**



DNA methylation levels at the age/stress-related *FKBP5* CpGs (cg20813374 and cg001305030) inversely correlate with *FKBP5* mRNA levels in breast tissue samples of control female subjects (n = 84). Publicly available data were analyzed from the Cancer Genome Atlas Wanderer (<http://maplab.imppc.org/wanderer/>). The x axis depicts the average % DNA methylation (Beta-values) of the CpGs. The y axis depicts log<sub>2</sub>-transformed normalized RSEM RNAseq-measured *FKBP5* expression.

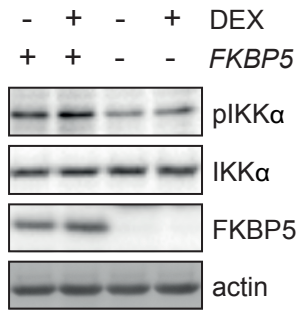
**Figure S7**



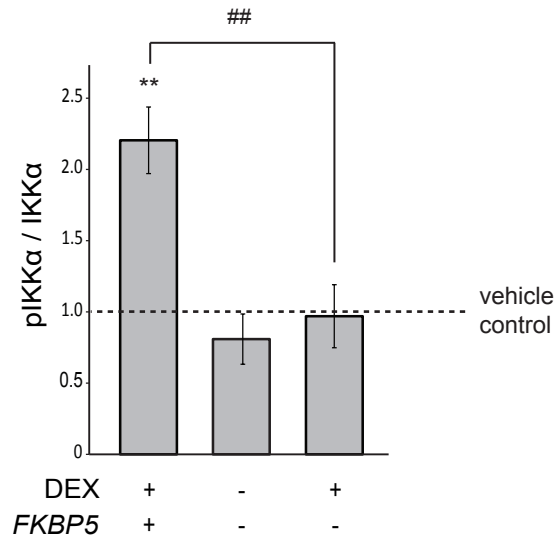
Association of *FKBP5* mRNA levels with the granulocyte to lymphocyte ratio (G/L), an inflammation marker linked with heightened cardiovascular risk and mortality in the Grady Trauma Project cohort (n = 330). The G/L was derived from Houseman-calculated blood cell proportions. Reported statistics and depicted residuals (on the x axis) are after correcting for age, sex, and the first two SNP-based principal components.

**Figure S8**

**A**



**B**



The effect of the stress hormone (glucocorticoid) receptor agonist dexamethasone (DEX) on functional phosphorylation of IKK $\alpha$  at serine 176 (pIKK $\alpha$ ) is abolished in Jurkat cells lacking *FKBP5*. *FKBP5* knockout cells were generated using CRISPR/Cas9 technology. **(A)** Representative Western blots in lysates of Jurkat cells with or without the *FKBP5* gene treated for 24 hours with DEX (100nM), which robustly induces *FKBP5* expression, or vehicle (DMSO). **(B)** Western blots were quantified, and pIKK $\alpha$  levels were normalized to total IKK $\alpha$  levels and are shown as fold changes in comparison to wild-type (*FKBP5* +) vehicle-treated cells. The treatment-genotype interaction was tested with two-way ANOVA ( $F_{1,8} = 8.1$ , interaction  $p = 2.2 \times 10^{-2}$ ,  $n = 3$  replicates per group) and significant effects were followed with Bonferroni-corrected pairwise comparisons. \*\*  $p < 10^{-2}$ , statistically significant pairwise comparisons for vehicle vs. DEX. ##  $p < 10^{-2}$ , pairwise comparisons for cells with (wild-type) vs. cells without *FKBP5* (knockout).



## Figure S9

*FKBP5* promoter, GRCh37/hg19 Assembly  
chr6:35,656,719-35,657,323 (antisense strand)

5'-GGCCTCTTCCTGTTTTAATCTCCTGGGATCTCCTGCTTGAAAGGTAGCAAGCCAA

GAGAAAGTATGGTCTTTACAGTCACTGGGTGTCCAGAGGGAGGTGATATCTGCTAAA

**NF-κB RE**  
TTGGTTCT**CG**AGGTGGGATTCCCCAGTCCCGACTGGGCATCTTAGACTTAATGGGG  
-484 -462

TTGCTTCCTAGGGCTAACCTGGCCAGCTGACCTAACAAACAGCCTGGCCTGCCCC-3'

380bp

*FKBP5* transcription start site

Annotation of the age/stress-related *FKBP5* CpGs and the constructs used to characterize their function. The figure shows in detail the 5'-3' sequence upstream of the *FKBP5* transcription start site of the DNA stretch (length 224 bp) that was inserted into the CpG-free luciferase reporter vector. The black bold letters highlight the sequence of the biotinylated probe (length 70 bp) used for the biotinylated oligonucleotide-mediated chromatin immunoprecipitation. The pink letters highlight the age/stress-related *FKBP5* CpGs. The underlined sequence and label highlight the NF-κB response element (NF-κB RE). As shown, both constructs include the CpGs and response element of interest, while they also completely lack other CpG sites to avoid non-specific CpG methylation effects.